A Biomimetic Wing-Actuation Mechanism for Micro Aerial Vehicles

Nathan Tardiff, Muhammad Shafiq Hanif Mohamad Hamdan, Ben Bradshaw, Keith Becker, Seyi Senbore, Su Cong, Haoxiang Luo[1]

Department of Mechanical Engineering, Vanderbilt University, Nashville, TN

ABSTRACT

We present a wing actuation mechanism and a prototype design for a flapping-wing micro air vehicle (MAV). The actuation design is based off of a two-wing system and features a single rotary motor and two sets of four-bar linkages, which allow the wings to flap and rotate around the wing-axis at the same time. A test rig and a two-wing prototype consisting of motor, linkage transmission, and flexible wings are constructed. High-speed imaging was used to analyze the instantaneous wing deformation. The frequency and force measurement were carried out.

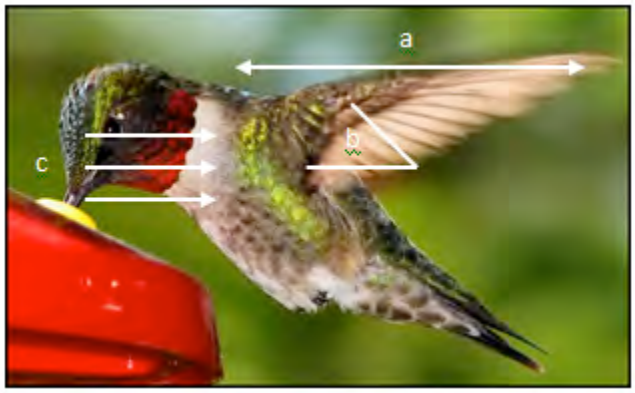

Figure 1: Diagram of stoke plane (a), incident angle of attack (b), and direction of relative airflow (c) for hovering hummingbird

1 INTRODUCTION

The development of micro air vehicles (MAVs) is motivated primarily by military use in intelligence, surveillance, and reconnaissance missions. The relatively small size seeks to hide the device from plain sight, achieve aerial agility, and operate in complex environments such as inside buildings. Due to their high maneuverability, many insects and small-size birds such as hummingbird have inspired a biomimetic approach for design of the MAVs. One of the key challenges for the flapping-wing MAVs is the wing actuation and control, whose mechanism obviously needs to be very efficient in terms of mass and energy. In this work, we propose a simple linkage mechanism for wing actuation, which allows the wing to rotate around its own axis while flapping. In addition, the structural design of the wing allows the wing to deform passively during flight. Such combined active/passive wing rotation is inspired based on the observation of the wing motions of insects and hummingbirds, and may produce high lift with potentially minimum amount of energy. In this paper, we will describe the actuation principle, wing design, and the prototype based on the wing mechanism.

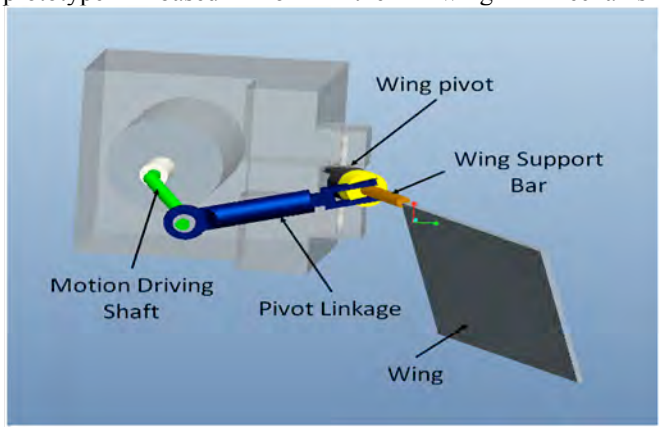

Figure 2: A design of flapping wing actuation mechanism. The mechanism is designed in 3D and can achieve both flapping and axial rotation at the same time. Only one-wing (arbitrary shape) is shown.

2 DESIGN COMPONENTS

2.1 Kinematic Design

The hummingbird was chosen to serve as a basis for kinematic design of the wing. High speed analysis of a hummingbird in hovering flight reveals that the stroke plane, defined as the plane in which the leading edge of the wing sweeps, is nearly parallel to the ground. During the forward half-stroke, the wing is rotated such that an angle of attack is established with respect to the relative airflow. The wing is rotated reversely during the backward half-stroke such that a similar angle of attack is established. This is a combination of active rotation, in which the animal physically rotates the wing, and passive rotation that results from the deformation of the wing. Figure 1 shows a diagram of the stroke plane and

[1] Corresponding author: haoxiang.luo@vanderbilt.edu

incident angle of attack during the forward stroke of a hovering hummingbird.

The key component in designing the mechanism was to incorporate active wing rotation such that if there is zero wing deformation, there would be an incident angle of attack between 0 and 90 degrees at all times throughout a complete wing stroke. The mechanism must also produce a simultaneous flapping motion, utilizing only one motor for power. Due to its simplicity, it was desired to utilize a 3D four bar linkage system to produce the desired 2-DOF system, as shown in Figure 2. This was accomplished by rotating the crank shaft using the motor, whose axis of rotation is parallel to the stroke plane of the wing bar. The coupler link transmits the motion into the flapping motion of the wing bar, and while changing the orientation, the coupler link also transmits an axial rotation to the wing bar. A schematic of the four-bar linkage system is shown in Figure 3. In this design, link 1 acts as the ground and link 2 represents the input link. It can be observed that the crankshaft rotates about the x axis and is the driving force of the mechanism. Link 4, the wing bar, is pinned to the fuselage. It is constrained such that it can only rotate in the x-z plane and also around its own axis. Hence, the x-z plane becomes the stroke plane for the mechanism. Link 3 connects links 2 and 4 and transmits the motion from the crank shaft to produce the desired wing bar kinematics.

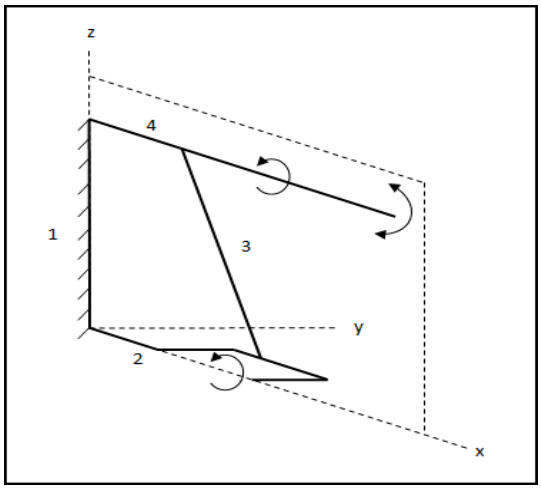

Figure 3: Schematic of 2-DOF four bar linkage system

The flapping motion produced by this mechanism can be analyzed by viewing the mechanism in the x-z plane, as shown in Figure 4. It is shown that the components of links 2 and 3 in the z-direction combine to control the motion of the wing bar. Since the length of link 1 is fixed, as this combined length changes it creates an angle, θ, which is referred to as the flapping angle. The total flapping angle is defined as twice the maximum flapping angle produced by the mechanism.

The wing bar rotation can be analyzed in a similar manner by viewing the mechanism in the y-z plane, as shown in Figure 5. In this figure, the wing bar would extrude out in the x-direction near the point in which links 1 and 3 intersect. Since the wing bar is constrained such that it can only produce a flapping motion in the x-z plane, as the components of links 2 and 3 move out of the stroke plane in the y-direction, they force the wing bar to rotate. The angle of rotation, ϕ, as seen in the diagram is referred to as the wing rotation angle. With a wing rigidly fixed onto the wing bar perpendicular to the stoke plane, this angle of rotation corresponds to the incident angle of attack with respect to the relative airflow as the wing flaps.

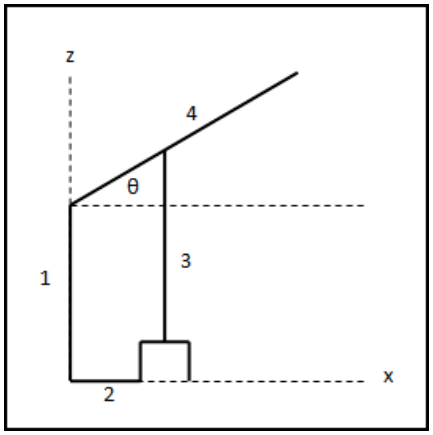

Figure 4: Diagram of flapping angle for 2-DOF system

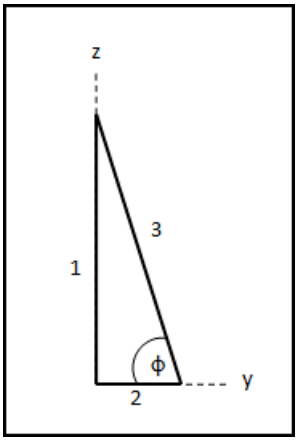

Figure 5: Diagram of wing rotation angle for 2-DOF system

With the general mechanism designed, the next step was to design each joint such that the mechanism would be properly constrained. Link 2 was designed as the crankshaft that would be coupled with the motor that drives the system. The motor would then be fixed to the base, as shown by connection (a) in figure 6. The most difficult connection is the joint between the crank shaft and link 3, shown by connection (b) in Figure 6. Due to the kinematics of the system, this joint requires three degrees of freedom. To varying degrees, link 3 must be constrained such that it can rotate about all three axes. The simply solution was to create a ball joint at this location, allowing for the 3 necessary degrees of freedom. The connection between link 3 and the wing bar, shown by (c), is a simple pin connection. Since this is only a 1-DOF connection, as links 2 and 3 move out of the stroke plane as previously discussed, the wing bar is forced to align with link 3.

The final connection, shown by (d), is the connection between the wing bar and the base. The two degrees of freedom sought by the mechanism as a whole are produced by

this connection as the wing bar will be rigidly attached to the wing. It was decided that the wing bar must be separated into two components, each with a different connection. A close-up of the connection is shown in Figure 7, where the orange wing bar and black hinge combine to form the entire wing bar. The first joint in the series, shown by (d_1), is a simply pin connection between the hinge and base. This constrains the two components of the wing bar to flapping in the x-z plane as previously described. The second joint, shown by (d_2) is a pin connection where the orange wing bar is free to rotate inside the hinge. This allows for the active wing rotation forced by the kinematics of the system. A cap on the end of the wing bar prevents it from moving axially inside the hinge, such that the connection is constrained for pure rotation.

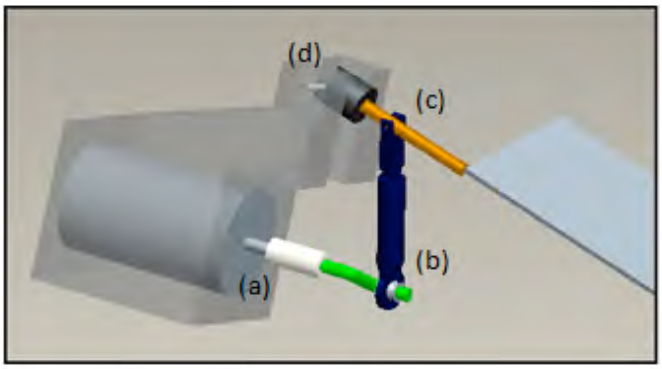

Figure 6: Diagram of connections for 2-DOF system

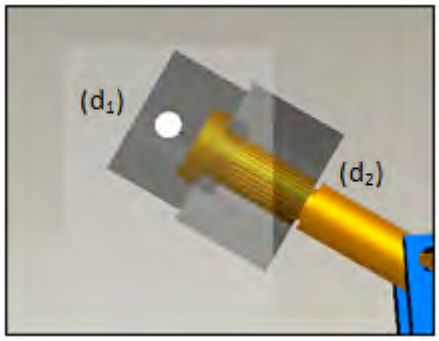

Figure 7: Close up of wing bar connections for 2-DOF system

The final step in the kinematic design of the mechanism was to dimension each link such that the wing exhibits the desired motion. After straightforward calculations, we set the distance between (d) and (c) as 0.75", as shown in Figure 9. The other key parameters shown in the figure are that X equals 1.637", Y equals 0.524", and Z equals 1.427". It should be noted that the referring to Figure 3 and Figure 4 that the x-distance between the connection of links 1 and 2 and the connection of links 2 and 3 was set to be 0.75". A Pro/E simulation confirmed that the design goals of approximately 15 degrees active rotation and a total flapping amplitude of approximately 100 degrees had been achieved, as shown in Figure 9 and Figure 10. It is observed in these plots that although the flapping angle and rotation angle do not exhibit pure sinusoidal behavior, they do represent symmetric oscillating signals as desired.

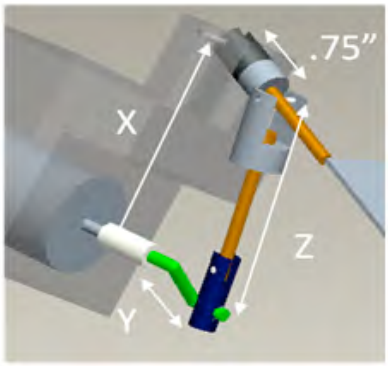

Figure 8: Primary dimensions for 2-DOF system

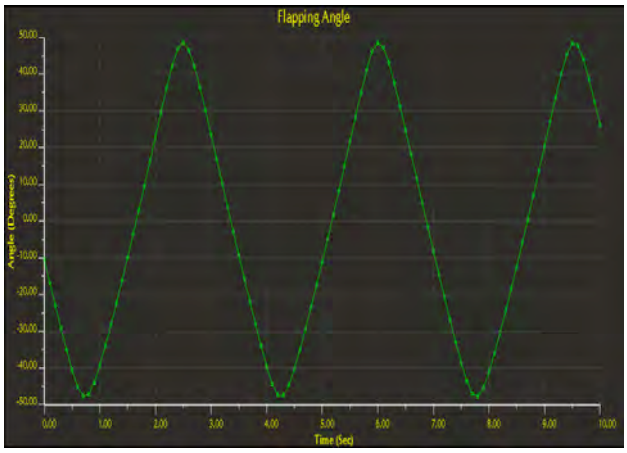

Figure 9: Plot of flapping angle for 2-DOF system

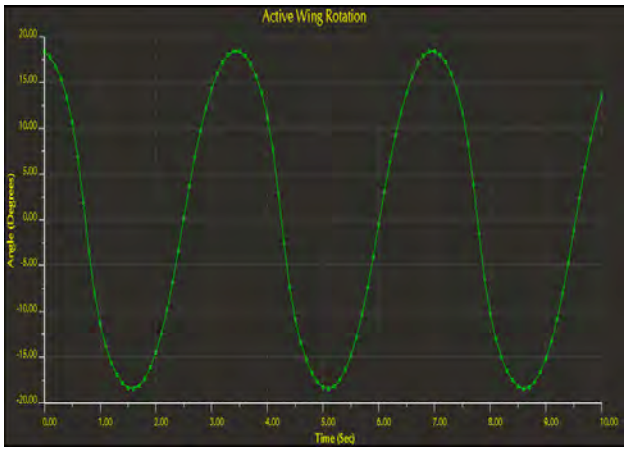

Figure 10: Plot of active wing rotation angle for 2-DOF system

2.2 Wing Design

The second stage of the flapping-wing MAV was to design the flexible wings that would enable the final prototype to achieve hovering flight. In parallel to the biomimetic design aspect of the final prototype, the wing design is based on wings of birds and insects found in nature that has hovering in mid air capabilities: dragonfly, hummingbird, and hawkmoth. Aerodynamics of insect flight has been discussed extensively in the literature[1]-[6]. The wing design focuses on obtaining favorable fluid-structure interaction and wing deformation that would enhance the lift and reduce drag. To achieve the goal, the flexibility of the wing frame should allow passive chord-

wise deformation that further reduces the wing angle of attack with respect to free-stream airflow in addition to the active rotation provided by the actuator mechanism (see Figure 11).

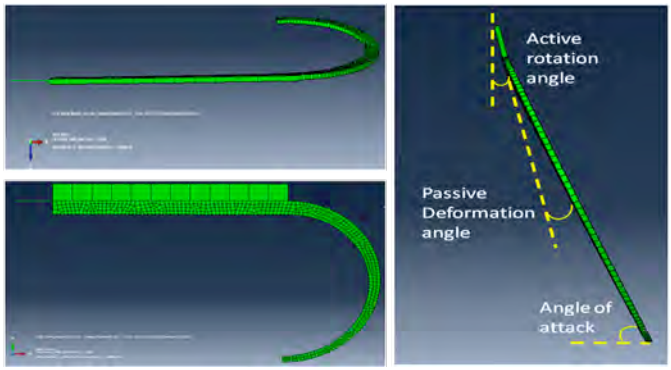

Figure 11: Front view (bottom left), top view (top left), and side view (right) of a deformed flexible wing frame without wing surface. The active rotation angle is produced by the flapping actuator mechanism. The passive deformation angle is a result of chord-wise deformation of the flexible wing. Larger active rotation angle and passive rotation angle both produces smaller angle of attack between wing and free-stream airflow

The basic shape of the wing design is based on the wing shapes of dragonfly, hummingbird, and hawkmoth. The actual shapes of the wings are simplified into a much simpler basic shape (see Figure 12) for practical purposes. Figures 13 to 16 show the simplified wing frames extracted from these three animals. For the wing materials, off-shelf carbon fiber sheets were used, and the wing frames were made from the sheets through the laser-cutting method. The wing surface is made from Mylar film (0.002") because it is very thin, lightweight, and strong enough to not easily tear under external forces. Also, the Mylar film has an adhesive backing on one side so that it can be easily placed onto the carbon fiber frame.

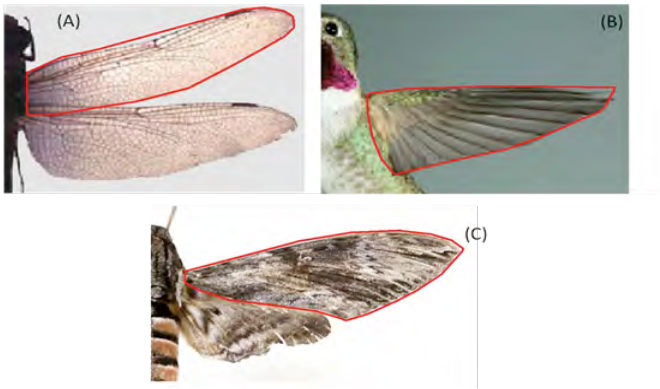

Figure 12: The red outline roughly defines the basic shape of dragonfly wing (A), hummingbird wing (B), and hawkmoth wing (C)

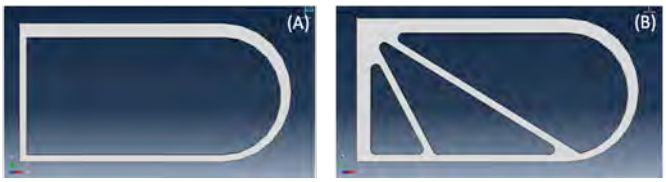

Figure 13: Dragonfly wing model without support bars (A) and with support bars (B)

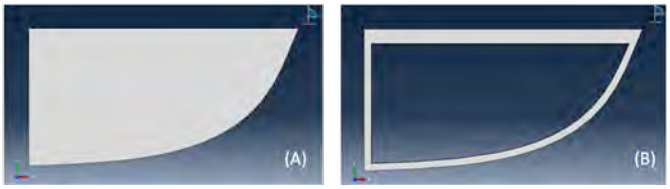

Figure 14: Hummingbird wing model basic initial shape (A) and without support bars (B)

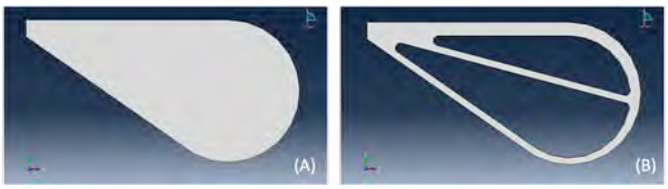

Figure 15: Hawkmoth wing model basic initial shape (A) and with support bars (B)

Figure 16: Final wing design based on hawkmoth wing. The black component is the wing frame with pin holes for mounting purposes. The wing frame is made of carbon fiber sheets. The translucent component is the wing surface made of a Mylar film.

After the basic wing shapes are dimensioned according to the design specifications, the inertial deformation of the wing frame is modeled in Abaqus software for structural analysis. The analysis led to the conclusion that the best basic wing shape is based on the hawkmoth wings.

2.3 Test Prototype

A test rig with only one wing was fabricated to test our theoretical results. The materials were selected and tested to perform at the desired frequency and range of motion. The test rig was run by an overly powerful test motor, to ensure we could generate enough torque to run the mechanism at high enough frequencies to see the wing deformation, and observe whether there was mechanism interference.

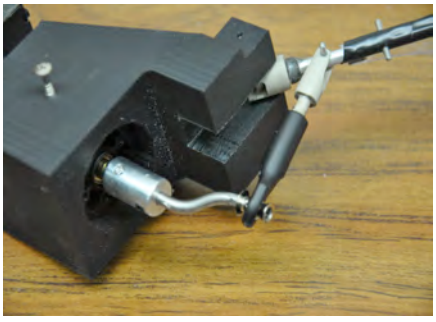

Figure 17: Assembled test rig mechanism

After building all of the parts to specifications and assembling them, we analyzed the results using an AMETEK Phantom v310 high-speed camera. While looking at the playback of several test runs, we were able to see our successes and failures in the design.

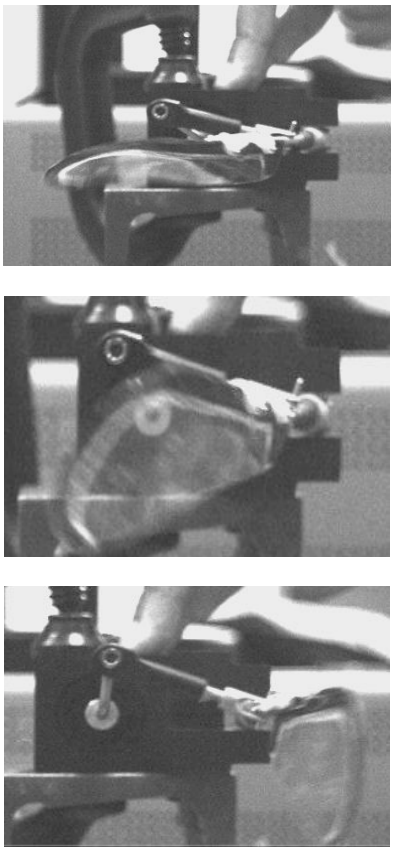

Figure 18: Motion of wing as seen through the AMETEK Phantom v310

Many of our design criteria were met, including the mechanism's active rotation and partial wing deformation. After showing playback of the motion of two wing designs, we observed irregular axial rotational motion for the smaller wing (wing chord length 5 cm). For the larger wing (wing chord length 7 cm), we observed a synchronized deformation pattern that is in phase with the flapping motion of the wing (Figure 18).

The load on the motor shaft during the flapping cycles has large fluctuations due to the inertial forces and the instantaneous locking positions of the linkage system. As a result, the motor speed of the test rig fluctuates. To overcome the problem, we used Simulink and an Arduino board to implement a PID controller that would run the system at a much more constant velocity.

2.4 Final Prototype Design and Fabrication

For the final prototype, the wing is made in the same way as the wing on the test rig, which includes a Mylar film surface and a carbon fiber frame laser-cut from the carbon fiber sheet (Figure 19). The wing bar material was chosen to be titanium. This is because this piece experiences very high stresses and so has to be strong. The clevis, and the wing bar hinges were all rapid prototyped using of ABS plastic. The ball joint with rod was purchased off the shelf. The gearbox and the motor for the final prototype were salvaged from an old RC helicopter (Figure 20). The assembled prototype with all parts is shown in Figure 21. The mount in the figure was rapid prototyped using ABS plastic.

Figure 19: Picture showing the carbon fiber cutout of the wing frame and the Mylar covering

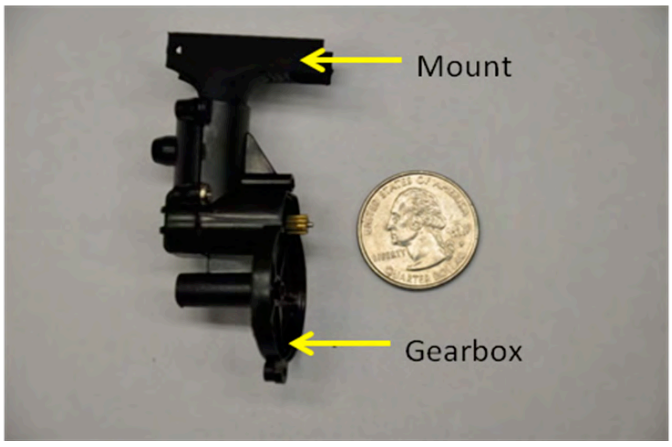

Figure 20: Picture showing 'the mount' attached to the salvaged motor and gearbox holder

#	Component	Fabrication Method
1	Gearbox + Motor	Repurposed
2	Mount	ME Rapid Prototyping
3	Ball Joint	Off-shelf
4	Hinge	SLA*
5	Clevice	SLA*
6	Wing Bar	Milling machine, slitting saw
7	Wing	Laser cutter, free-form cut
8	Stand	Repurposed

*Stereolithography Apparatus (SLA) Done by ACU-Cast Tech. LLC

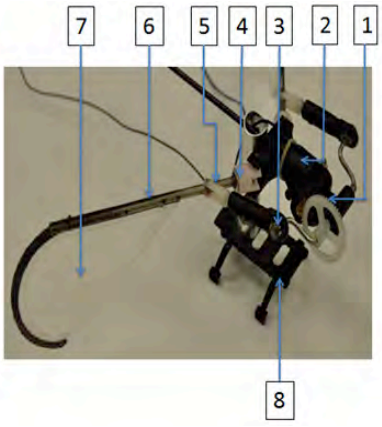

Figure 21: Figure showing all the parts and their fabrication method (the other wing is not shown in the picture)

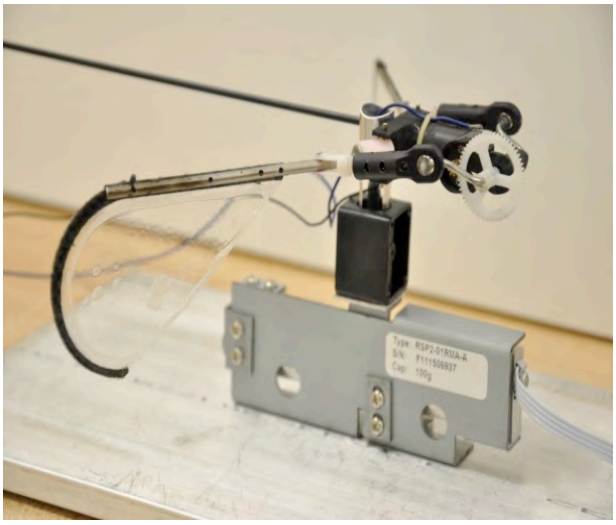

Figure 22: The MAV prototype attached to a load cell for the force measurement

2.5 Test of Flapping Motion and Lift Measurement

Experimental testing of the prototype ornithopter was done with the prototype fixed on a load cell (Loadstar Sensors, CA) and connected to a power supply (Figure 22). The input voltage was measured, and the frequency was determined using the high-speed camera setup, examining the average rate of 10 flaps taken at a speed of 500 FPS. Two wings were tested; a 5 cm chord length wing and a 6 cm. Four voltages were tested for the 5 cm wing while 2 voltages were tested for the 6 cm. Each voltage's corresponding set of force data was averaged to find the lift force over an interval of 0.250 seconds at a sampling frequency of 4000 Hz.

The measured flapping frequency is shown in Figure 23. It can be seen that there is a frequency increase as the voltage is raised, as expected. A maximum frequency around 10 Hz was achieved. Higher frequencies may lead to burnout of the motor. The instantaneous lift of the prototype with and without the wings mounted is shown in Figure 24. Due to the high inertial force and vibration of the prototype, the average lift calculated from the force history is insignificant.

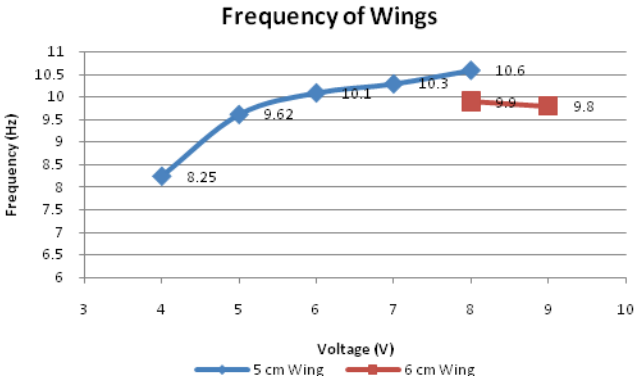

Figure 23: Frequency of wings vs. voltage of the final prototype

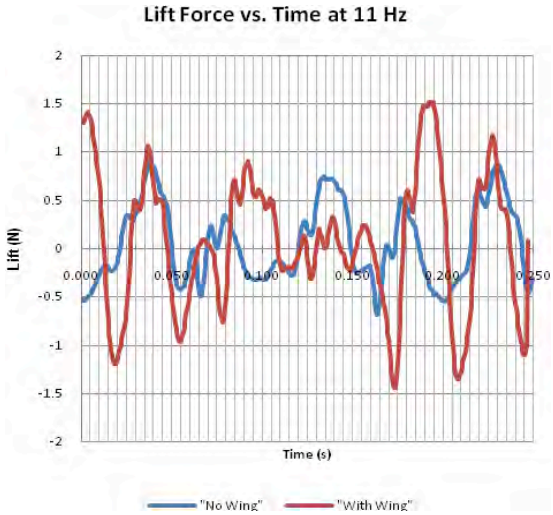

Figure 24: Lift force as measured at a frequency of 11 Hz both with and without wings

3 CONCLUSION

We have designed a wing actuation mechanism for flapping wing MAVs, which allows the wing to rotate around its own axis while flapping. Such wing kinematics with two angles of rotation is inspired from insects and hummingbirds and has potential to produce higher lift compared with the wings that have only flapping motion. We have constructed a single-wing test rig and also a two-wing prototype to demonstrate the feasibility of the mechanism. A flapping frequency of 10 Hz was achieved for the prototype. For the future design, improvement of the structural design of the machine parts and further reduction of the mass are needed to decease the force oscillation due to inertia of the moving parts. In addition, the parts should be more precisely machined to reduce vibration.

4 ACKNOWLEDGEMENT

The material is based on a Senior Design project sponsored by the Air Force Research Laboratory under agreement number FA8650-09-2-7929.

REFERENCES

[1] Ansari, S.A.; Knowles, K.; Zbikowski, R. "Insectlike Flapping Wings in the Hover Part 1: Effect of Wing Kinematics" Journal of Aircraft, vol. 45, pp. 1945-1954, (2008)

[2] Singh, B.; Inderjit, C.; Manikandan R.; Leishman, J.G. "Experimental Studies on Insect-Based Flapping Wings for Micro Hovering Air Vehicles", *46th AIAA Structures, Structural Dynamics & Materials Conference, Austin, Texas*, AIAA 2005-2293, (2005)

[3] Dickinson, M.H.; Lehmann, F.O.; Sane, S.P. "Wing Rotation and the Aerodynamic Basis of Insect Flight", *Science*, vol. 284, pp. 1954-1960, (1999)

[4] Lehmann, F.O. "The mechanisms of lift enhancement in insect flight", *Naturwissenschaften*, vol. 91, pp. 101-122, (2004)

[5] Sane, S.P. "Review: The aerodynamics of insect flight", *The journal of Experimental Biology*, vol. 206, pp. 4191-4208, (2003)

[6] Lehmann, F.O. "Review: When wings touch wakes: understanding locomotor force control by wake-wing interference in insect wings", *The journal of Experimental Biology*, vol. 211, pp. 224-233, (2008)